

Submitted to Environmental Science and Technology, May 31 2012

**Simultaneous release of Fe and As during the reductive dissolution of Pb-As
jarosite by *Shewanella putrefaciens* CN32**

Christina M. Smeaton^{1,2}, Gillian E. Walshe^{1,3}, Adrian M.L. Smith^{4,5,6},*

Karen A. Hudson-Edwards⁶, William E. Dubbin⁴, Kate Wright^{5,7}, Andrew M. Beale^{5,8},

Brian J. Fryer¹ and Christopher G. Weisener¹

¹ Great Lakes Institute for Environmental Research, University of Windsor, Windsor, Ontario N9B 3P4, Canada.

² Ecohydrology Research Group, Department of Earth and Environmental Sciences, University of Waterloo, Waterloo, Ontario, Canada, N2L 3G1.

³ Current address: Department of Microbiology, University of Tennessee, Knoxville, Tennessee, 37996, USA.

⁴ Department of Mineralogy, The Natural History Museum, Cromwell Road, London, SW7 5BD, UK.

⁵ Davy Faraday Research Laboratory, The Royal Institution of Great Britain, 21 Albemarle Street, London, W1S 4BS, UK.

⁶ Department of Earth and Planetary Sciences, Birkbeck, University of London, Malet Street, London, WC1E 7HX, UK.

⁷ Current address: Nanochemistry Research Institute, Department of Chemistry, Curtin University, GPO Box U1987, Perth, WA 6845, Australia.

⁸ Current address: University of Utrecht, Debye Institute, Department of Inorganic Chemistry and Catalysis, Sorbonnelaan 16, 3584 CA Utrecht, The Netherlands.

SUPPORTING INFORMATION

MANUSCRIPT:

N° of pages: (18 pages of text plus 4 pages for the Table, the figures, and the brief)
N° of figures: 3

SUPPORTING INFORMATION:

N° of pages: 20 (including cover page, 5 pages of text, 3 pages of tables, 10 pages of figures)

N° of figures: 10

N° of tables: 6

S1. Bacterial cultivation method

Pure cultures of *Shewanella putrefaciens* were prepared from 1.5 mL frozen glycerol stocks maintained at -80 °C and transferred to Trypticase Soy Agar (TSA) plates and grown aerobically for 24 hours. Single colonies were inoculated into 25 mL of sterile Trypticase Soy Broth (TSB) and incubated aerobically at 32 °C for 16 hours. Seed cultures (10 mL) were used to inoculate 4 x 100 mL aliquots of sterile Luria-Bertrani (LB) media and incubated aerobically at 32 °C until the culture reached late log phase (16 hours). Bacteria were harvested by centrifugation at 3000 rpm for 20 minutes and washed twice using sterile 0.01M NaNO₃, decanting the supernatant and centrifuging at each step. Wet biomass was washed once using 100 mL of N₂ purged minimal media. The minimal media was decanted and the cells were suspended in 1.0 L of media with a final wet mass of 1.08 g/1 L of media. All solutions were prepared from ACS grade reagents and were either filter sterilized (0.2 µm) or autoclaved.

S2. ATP Analysis

Briefly, 150 µL of the BacTiter-Glo™ reagent was added to 150 µL of a sample slurry, shaken for 5 minutes and luminescence was measured using a GloMax® 20/20 Single Tube Luminometer (λ 350-650 nm) at an integration time of 2 seconds and the output was reported in relative luciferase units (RLU). Control samples were also analyzed to determine the intensity of the luminescent signal produced by the minimal media and the Pb-As jarosite in the absence of *S. putrefaciens*. The RLU values were converted to ATP concentrations using the average of

three calibration curves prepared with an ATP standard in minimal media (10 mM; Promega Corporation).

S3. TEM preparation and analysis

The primary fixative used for TEM samples preparation was 0.2M glutaraldehyde (2% v/v) in 0.1M phosphate buffer at pH 6.8. Samples were rinsed 2X in the buffer solution, post-fixed in 1% osmium tetroxide in 0.1M phosphate buffer for 1 hour. A graded ethanol series followed (50%, 70%, 70%, 95%, 95%, 100%, 100%) and final dehydration was completed in 100% propylene oxide (PO). Spurr's resin was used to infiltrate samples in a series (2:1 PO:Spurr's, 1:1 PO:Spurr's, 1:2 PO:Spurr's, 100% Spurr's, 100% Spurr's, 100% Spurr's). Samples were transferred to embedding moulds, filled with fresh 100% Spurr's resin and left overnight at 60°C. Thin sections (Leica UCT Ultramicrotome) were placed onto both uncoated grids and some Formvar-coated grids and samples were lightly carbon coated (10-15 Å). Specimens were examined using field emission- transmission electron microscopy (FE-TEM) (FEI Titan 80-300). Bright field (BF) images and high angle annular dark field (HAADF) scanning transmission electron microscopy (STEM) images.

S4. X-ray Absorption Spectroscopy (XAS)

Absorption spectra were collected at room temperature in transmission mode using a 13 element solid state Ge-detector from -200 (pre-edge) to +1000 eV (post-edge) of the As (11 867 eV) and Fe (7110.75 eV) K-edges. The energy of the Si(111) double crystal monochromator was calibrated using an Au foil and each standard/ sample was scanned 3-4 times. Proportions of As(III)/As(V) and Fe(II)/Fe(III) were determined by linear least squares combination fitting of

the XANES spectra using the spectra of As(III) as sodium meta-arsenite (NaAsO_2), As(V) as the pure Pb-As-jarosite, Fe(II) as wustite (FeO) and Fe(III) as the pure Pb-As-jarosite as standards.

Extended X-ray Absorption Fine Structure (EXAFS) data for the original Pb-As jarosite were collected at the CLRC Synchrotron Radiation Source at Daresbury Laboratory, UK, which operates at 2 GeV with a typical current of 150 to 250 mA. X-ray absorption spectra were collected at the Fe and As K-edges (7.12054 and 11.8695 keV) on station 9.2 which was equipped with a Si(111) double crystal monochromator, and ion chambers for measuring incident and transmitted beam intensities. 10 μm Fe and As foils were used to calibrate the monochromator position. In order to reduce the presence of higher harmonics the focused beam was detuned by approximately 50 %. The sample was mounted as a pressed pellet (diluted with diffused silica, $\varnothing 15\text{mm}$) on to a liquid nitrogen cryostat (80 K) and between 7-10 quick (Q)EXAFS data scans were collected for each sample at both edges. XAS data were processed using EXCALIB, EXBSPLINE and EXCURV98.¹

S5. Arsenic Speciation Method

For As(V), 100 μL of a color reagent was added to 900 μL of the acidified sample and analyzed following a 30 minute reaction period. The color reagent contained 0.613 M L-ascorbic acid ($\text{C}_6\text{H}_8\text{O}_6$), 24 mM ammonium molybdate ($[\text{NH}_4]_6\text{Mo}_7\text{O}_{24}$), 8 mM potassium antimonyl tartrate ($\text{C}_8\text{H}_4\text{K}_2\text{O}_{12}\text{Sb}_2 \cdot 3\text{H}_2\text{O}$) and 2.5 M sulphuric acid (H_2SO_4). The aforementioned color reagent solutions were prepared separately and mixed in a 2:2:1:5 ratio (by volume) in the order listed. Special care was taken to prevent turbidity in the coloring reagent by adding the H_2SO_4 immediately following the addition of the first 3 reagents. Absorbance was measured using a GENESYS 20 UV-VIS Spectrophotometer at 873 nm. Total arsenic was determined by adding

100 μL of an oxidizing reagent to 900 μL of the sample. The oxidizing reagent contained 2 mM potassium iodate (KIO_3) in 2% v/v HCl. Samples were heated at 95°C for 10 minutes in a wellled hot-plate and cooled on ice for 5 minutes. Following cooling, 100 μL of the color reagent was added to the sample and the absorbance was measured. Arsenite and arsenate concentrations were determined using calibration curves of sodium arsenate ($\text{Na}_2\text{HAsO}_4 \cdot 7\text{H}_2\text{O}$) and sodium *m*-arsenite (NaAsO_2) stock solutions and were matrix matched with experimental samples and contained minimal media, 1% v/v HCl and 1 μM KH_2PO_4 . Arsenite and arsenate detection limits were 6.25 and 0.625 μM , respectively. As(III) concentrations were determined by subtracting As(V) from total arsenic. Total As concentrations determined in this method were compared to ICP-OES As totals and were within the standard errors of each measurement at each time interval.

S6. EXAFS analysis of the original Pb-As jarosite

Fitting of the EXAFS data for the Pb-As jarosite was performed in k-space using curved wave theory and in accordance with previous work both single and multiple scattering events (using Rehr-Albers small atom theory) were considered.²⁻⁴ Specifically for the multiple scattering calculations a cluster was constructed with C1 symmetry that was based on the local structure around a sulfur site in jarosite, derived from the crystal structure.⁵ In order to ensure that the number of refineable parameters did not exceed the number of experimental observations, coordination numbers were constrained to a value of 1 and the Debye-Waller factors of similar types of scattering species were grouped together.⁶ Bond lengths and bond angles around the cluster were refined in order to obtain detailed information on the local structure around the arsenic site and the refinement that yielded the best fit of the data whilst retaining chemically sensible bond distances between the nearest neighbours.

The fitted Fe K-edge EXAFS spectra and associated FT for the Pb-As-jarosite sample are shown in SI Figure S10 and the derived parameters are listed in Table S7. The results from a first shell analysis suggested that the Fe species in the sample existed as Fe(III) in octahedral coordination. It is known from crystallographic studies of jarosite that the Fe site is distorted and therefore contains four equatorial oxygens at a distance of 1.97 Å and two axial oxygens at 2.06 Å.⁷ The EXAFS technique is unable to resolve these two different contributions but a bond distance of 2.01 Å can be rationalised as being an average of 4×1.97 Å and 2×2.06 Å. In the structure two of the equatorial oxygens corner share with other FeO₆ octahedra whilst the remaining two bind to hydrogen. The axial ligands coordinate to the interconnecting sulfur species which we observe at a distance of 3.25 Å away. The As that is substituting for some of the S sites is located at a slightly longer distance from the Fe of 3.31 Å.⁸ The identification of a shell of four Fe atoms at a distance of 3.67 Å is also typical of the jarosite structure.

A simple first shell analysis of the As data yielded four oxygens at an average distance of 1.69 Å (Table S7) and is consistent with the presence of tetrahedral As(V) species in the structure. Further proof for the substitution of As for S within the structure and a more detailed picture of the local coordination around the As substituent, was obtained by fitting the higher shells and by considering multiple scattering events. A best fit of the higher shell data was obtained in which three Fe species were observed at distances of 2.87, 3.34 and 3.38 Å, respectively (Table S7). The contribution of oxygen atoms at distances around 3.40 Å were found to be negligibly small owing to a large static disorder (large Debye–Waller factors) and therefore excluded from the model.

Table S1. Gibbs Free Energy of Formation for Reaction Constituents

Constituent	ΔG°_f (kJ/mol)
Pb ²⁺	-24.2 ⁹
Fe ³⁺	-16.28 ¹⁰
Fe(OH) ₂ ⁺	-438 ¹¹
Fe ²⁺	-91.5 ¹⁰
SO ₄ ²⁻	-744.46 ¹²
HS ⁻	11.97 ¹³
C ₃ H ₅ O ₃ ⁻	-512.67 ¹³
C ₂ H ₃ O ₂ ⁻	-369.33 ¹³
HAsO ₄ ²⁻	-713.73 ¹⁴
H ₃ AsO ₃	-640.03 ¹⁴
HCO ₃ ⁻	-586.94 ¹³
H ₂ O	-237.18 ⁹
Pb-As jarosite	-3041.64*

*calculated in this study.

Table S2. Measured chemical parameters and log activities used in React (GWB 7.01) for the control and inoculated Pb-As jarosite samples at 336 hours.

Component	Treatment			
	Control	Log activity	Biotic	Log activity
Fe ³⁺ (as Fe(OH) ₃)	20 μM	-4.75	---	---
Fe ²⁺	---	---	2166 μM	-2.99
Pb ²⁺ (as PbCO ₃)	5 μM	-5.82	5 μM	-5.31
SO ₄ ²⁻	109 μM	-4.25	1040 μM	-3.31
Cl ⁻	30 mM	-1.55	30 mM	-1.56
CH ₃ CH(OH)COO ⁻	24 mM	-1.69	19 mM	-1.80
CH ₃ COO ⁻	---	---	566 μM	-3.41
HCO ₃ ⁻	---	---	566 μM	-3.36
HAsO ₄ ²⁻	20 μM	-5.05	191 μM	-4.07
H ₃ AsO ₃	---	---	50 μM	-4.31
pH	7.40	-7.40	7.42	-7.42
Eh	+243 mV	---	-104.9 mV	---

Table S3. Predicted saturation indices (log Q/K) of potential secondary precipitates using calculated activities of control and inoculated Pb-As jarosite samples at 336 hours.

Mineral	LogK*	Treatment	
		Control	Inoculated
Hematite	0.0433	14.50	---
Schwertmannite	18	9.68	---
Goethite	0.4999	6.77	---
Fe(OH) ₃	4.889	2.38	---
Pb ₃ (AsO ₄) ₂	-35.384	-0.55	---
Anglesite	-7.8138	-2.25	---
Vivianite	-11.3774	---	5.29
Siderite	-0.2214	---	1.28
Fe(OH) ₂	12.8485	---	-1.00
Cerrusite	-3.1856	---	-1.75

* Delaney, J. M.; Lundeen, S. R. *The LLNL thermochemical database*; UCRL-21658; Lawrence Livermore National Laboratory: 1990; p 150.

Table S4. Locations of spectra collected during TEM-EDX analysis and corresponding relative elemental concentrations reported in weight %

Element	Spectra (wt%)			
	1	2	3	4
O K	38	39	37	36
Fe K	32	25	32	38
As K	---	20	31	---
Pb L	23	16	---	18
S K	7	---	---	8

Table S5. SEM-EDS Analysis of relative elemental weight percent and standard deviation (n=3) of bulk Pb-As jarosite at randomly selected areas over time

Element	Time 0		168 hours		336 hrs	
	Wt %	S.D	Wt %	S.D	Wt %	S.D
OK	41	2	36	1.2	43	1.8
SK	13	0.8	10	1.5	9	0.4
FeK	28	2	32	0.7	25	1
AsK	1	0.2	5	0.5	2	0.8
PbL	17	0.5	16	3	21	1.3

Table S6. Parameters derived from the EXAFS fitting of the Fe and As K-edges shown for the Pb-As-jarosite sample.

Edge	Shells	N	R (Å)	$2\sigma^2(\text{Å}^2)$	Angle As-O-Fe	R (%)
Fe-K	O	6	2.01	0.016		22.89
	S	1.61	3.25	0.012		
	As	0.4	3.31	0.005		
	Fe	4	3.67	0.021		
As-K	O	2	1.69	0.005		26.67
	Fe	1	2.87	0.018	101	
	Fe	1	3.34	0.010	127	
	Fe	1	3.38	0.010	130	

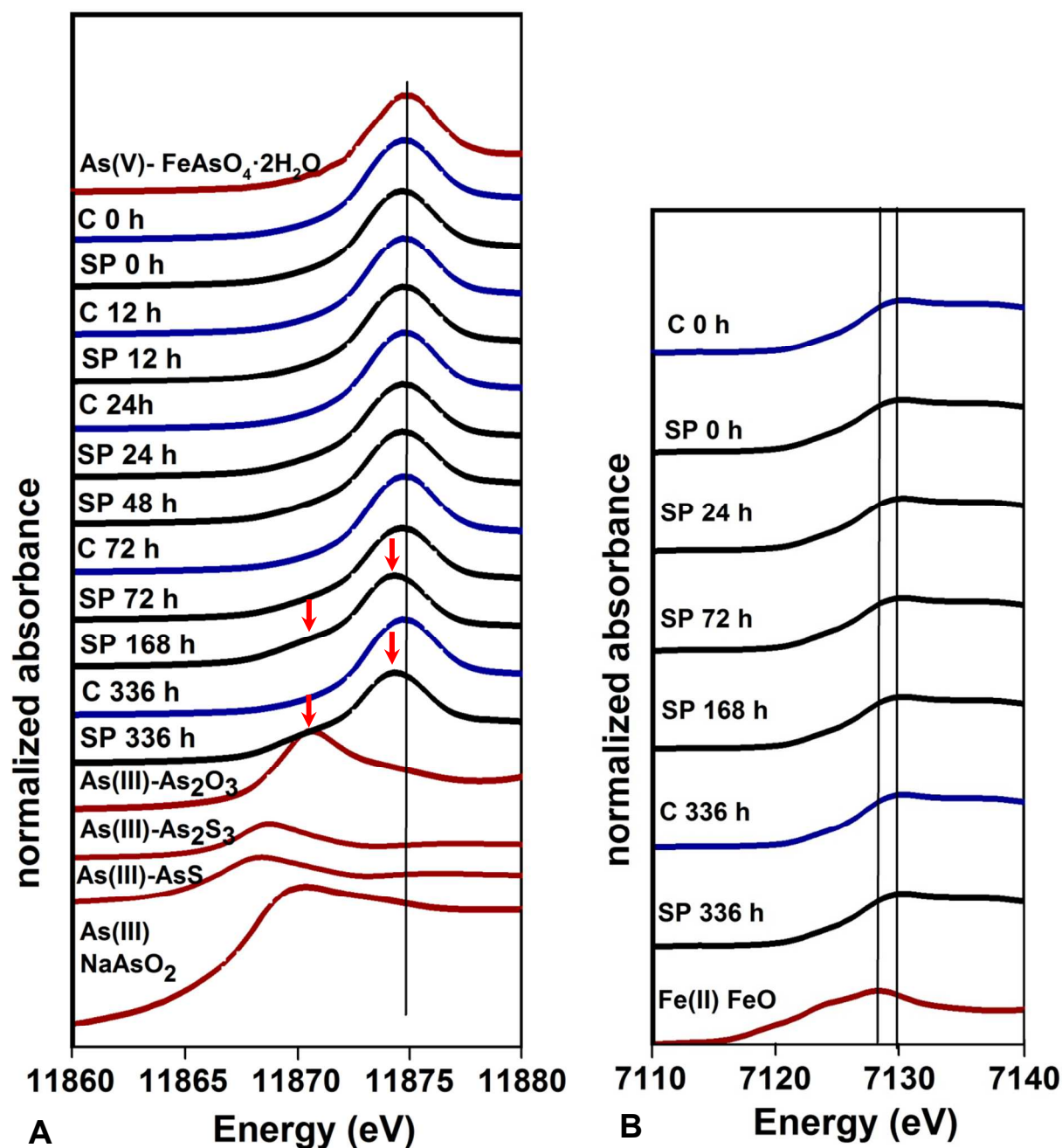


Figure S1. Comparison of A) As-K and B) Fe K-edge XANES spectra on standards (red line), inoculated (black line) and control (blue line) Pb-As jarosite samples over time. Red arrows in (A) mark the shift in the As-K edge in inoculated samples and the emergence of an As(III) shoulder at 168 and 336 hours. Note: the inoculated data corresponds to the same spectra presented in Figure 2 of the main document

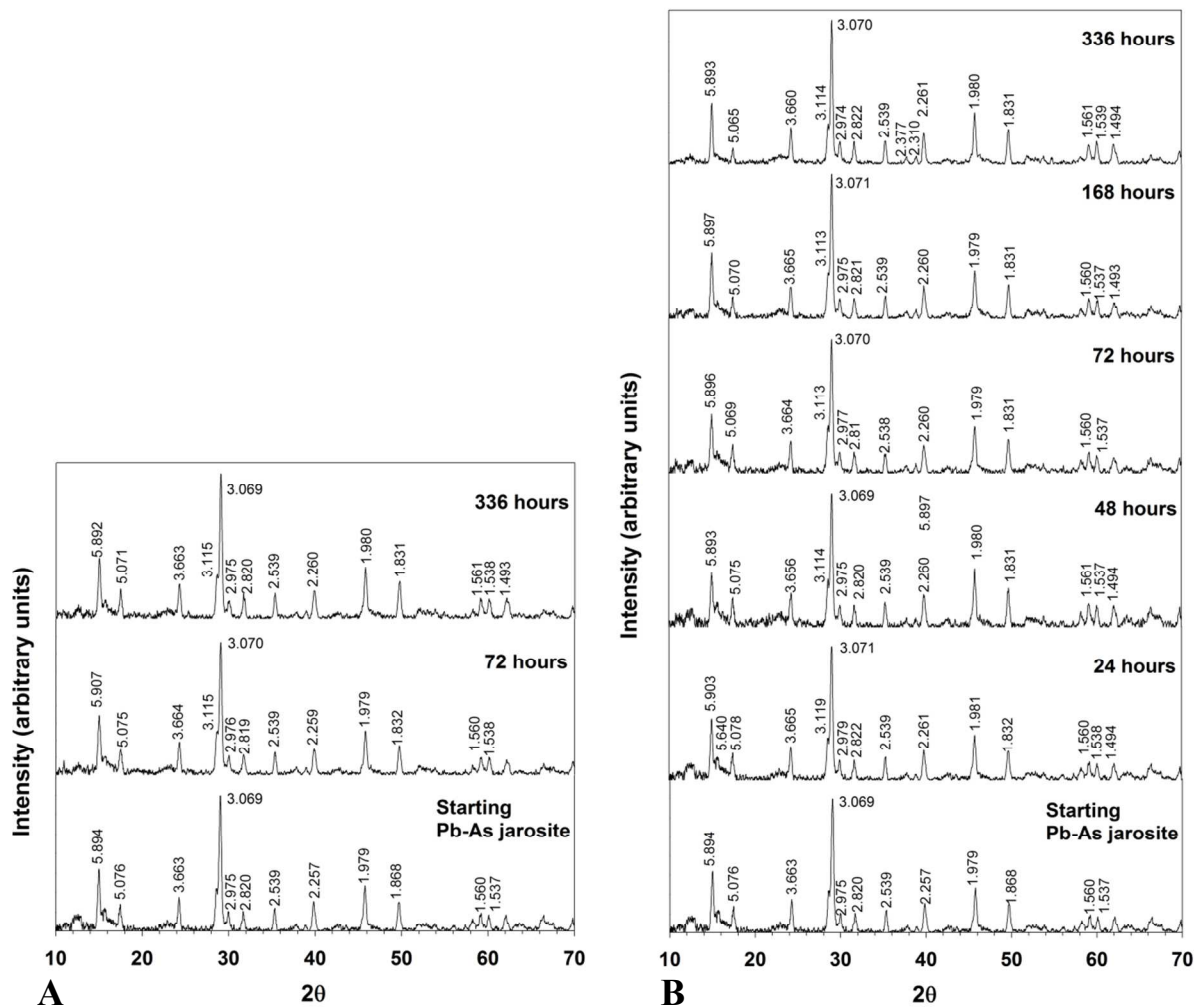


Figure S2. Powder X-ray diffraction patterns of A) control, and B) inoculated Pb-As jarosite samples taken at selected time intervals.

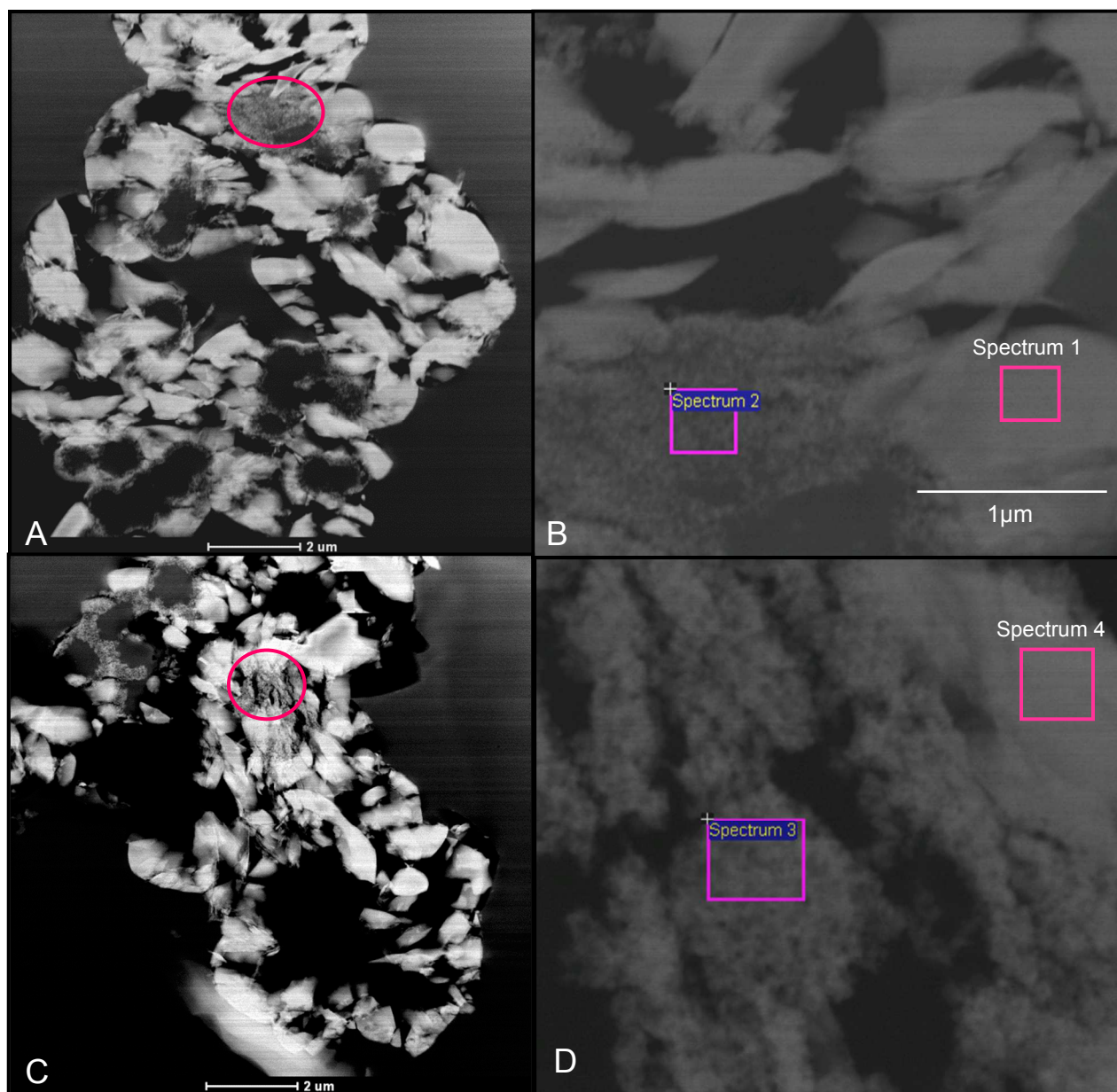


Figure S3. Dark field TEM images of control Pb-As jarosite samples at 336 hours. Ovals correspond to the area of secondary precipitates magnified in images B and D. Spectrum numbers in B and D denote areas of EDS analysis corresponding to Table S5 and EDS spectra in Figure S3.

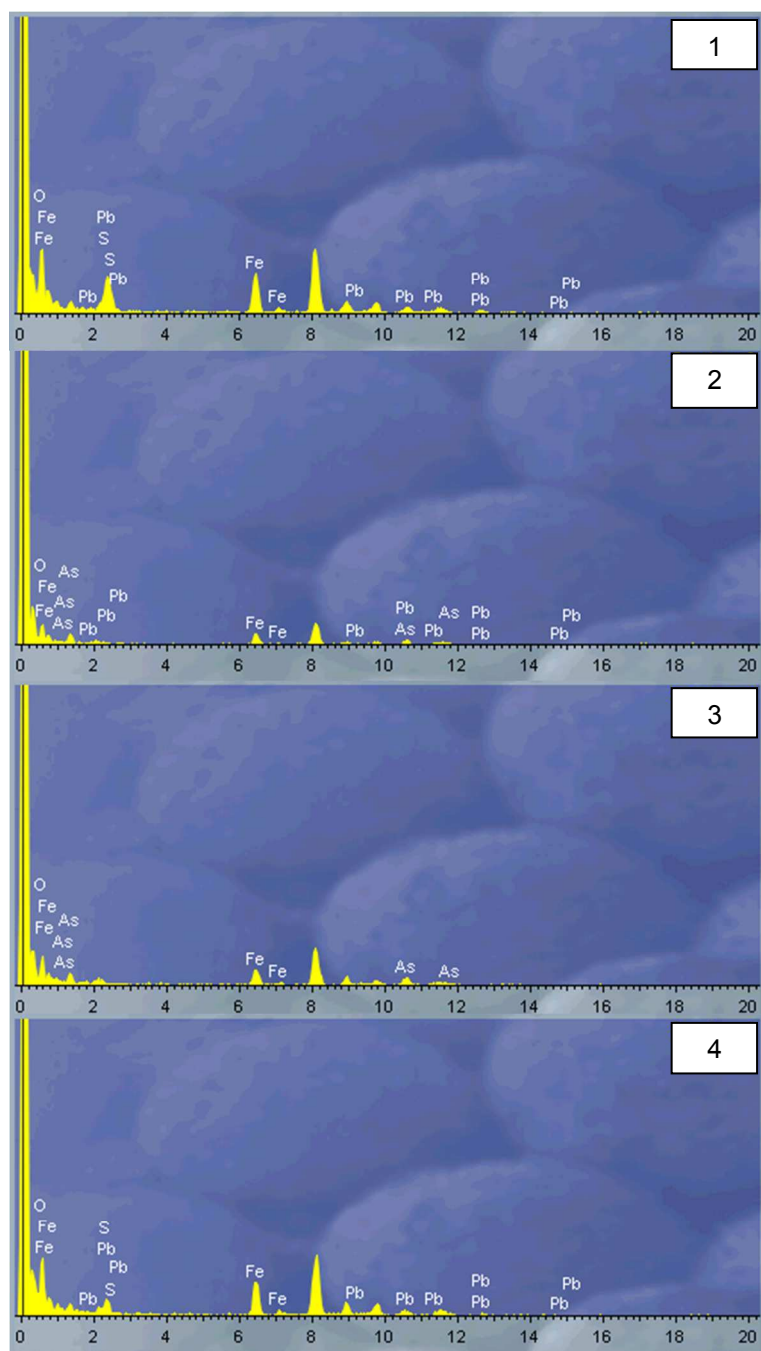


Figure S4. Corresponding EDS spectra of areas denoted as Spectrum 1, 2, 3 and 4. Note: C and Cu peaks at 1 and 8.01 keV were not labeled due to contribution from formvar grids and carbon coating.

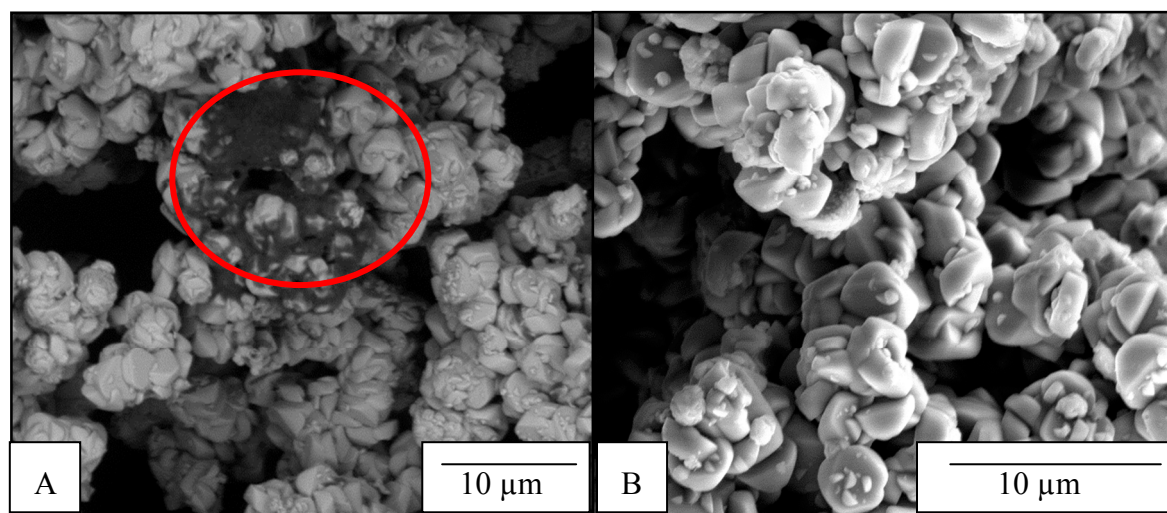


Figure S5. A) BSE-SEM image of inoculated Pb-As jarosite at 0 h and B) SE-SEM image of inoculated Pb-As jarosite at 336 hours. The dark rods within the circle are *S. putrefaciens* cells.

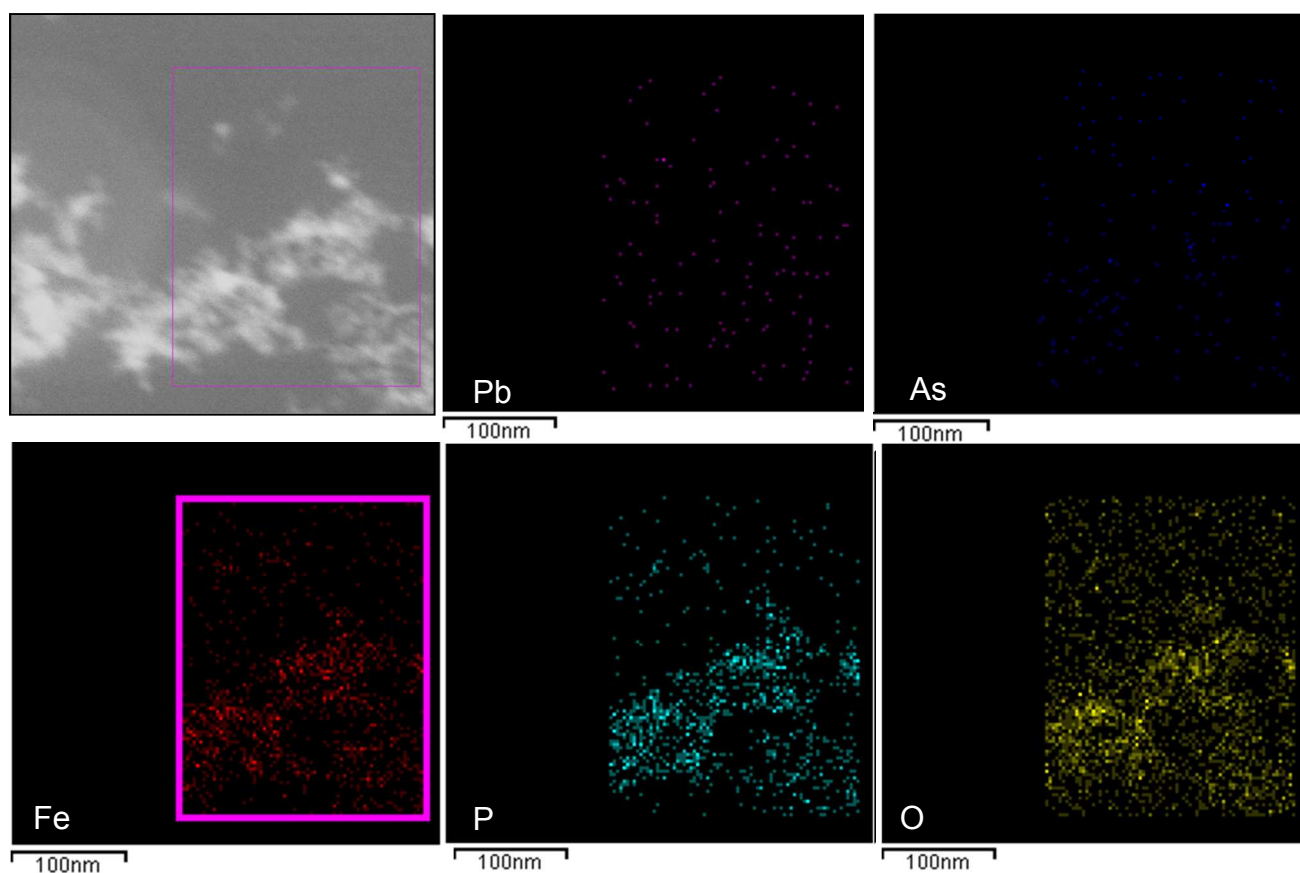


Figure S6. TEM-EDS elemental maps of secondary precipitates in the inoculated Pb-As jarosite sample at 336 hours.

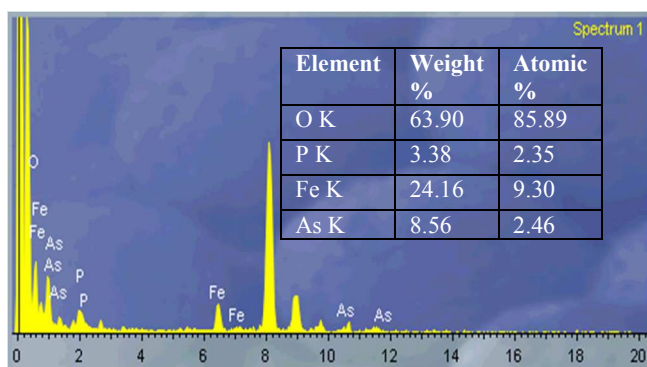
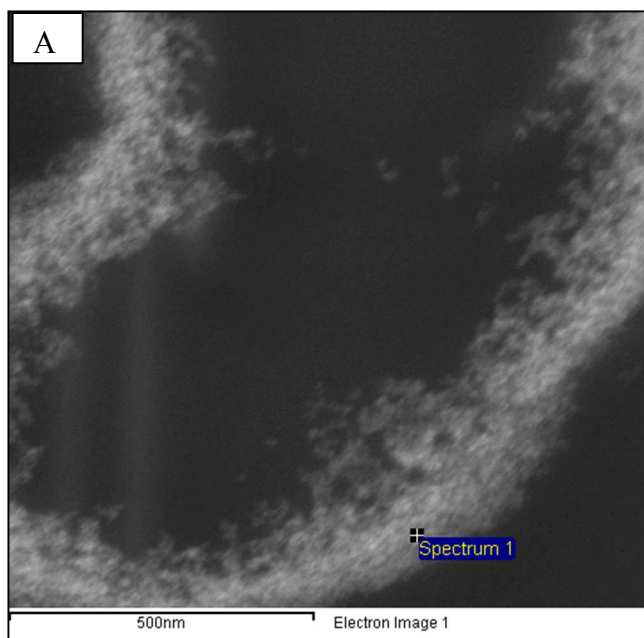


Figure S7. A) STEM image of secondary precipitate taken at 336 hours, and B) EDS spectra of area labeled Spectrum 1 and the inlaid table is the relative wt% and at% elemental concentrations of O, P, Fe and As. Note: C and Cu peaks at 1 and 8.01 keV were not labeled due to contribution from formvar grids and carbon coating

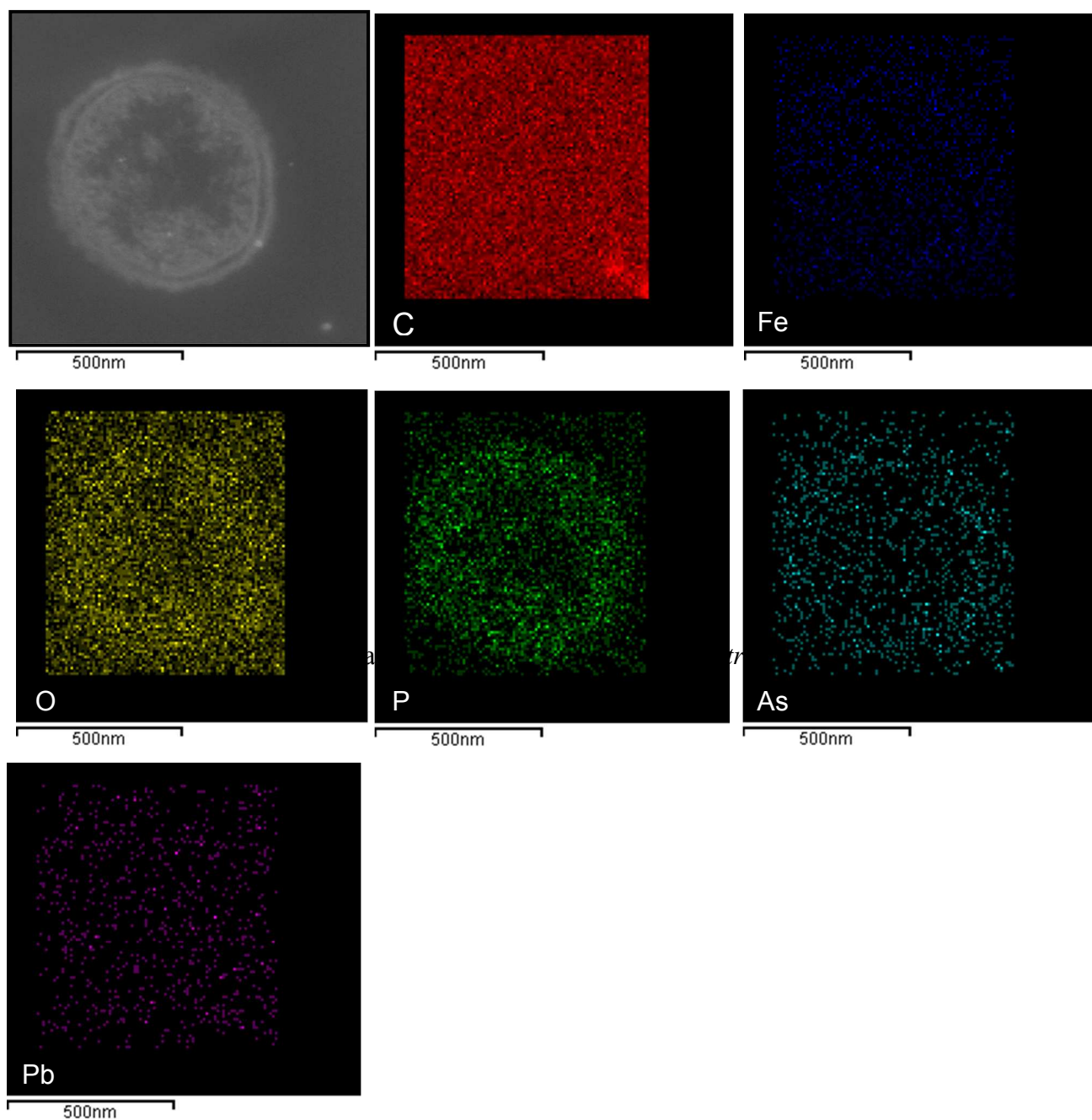


Figure S8. TEM-EDS elemental maps of a cross sectioned *S. putrefaciens* cell at 0 hours.

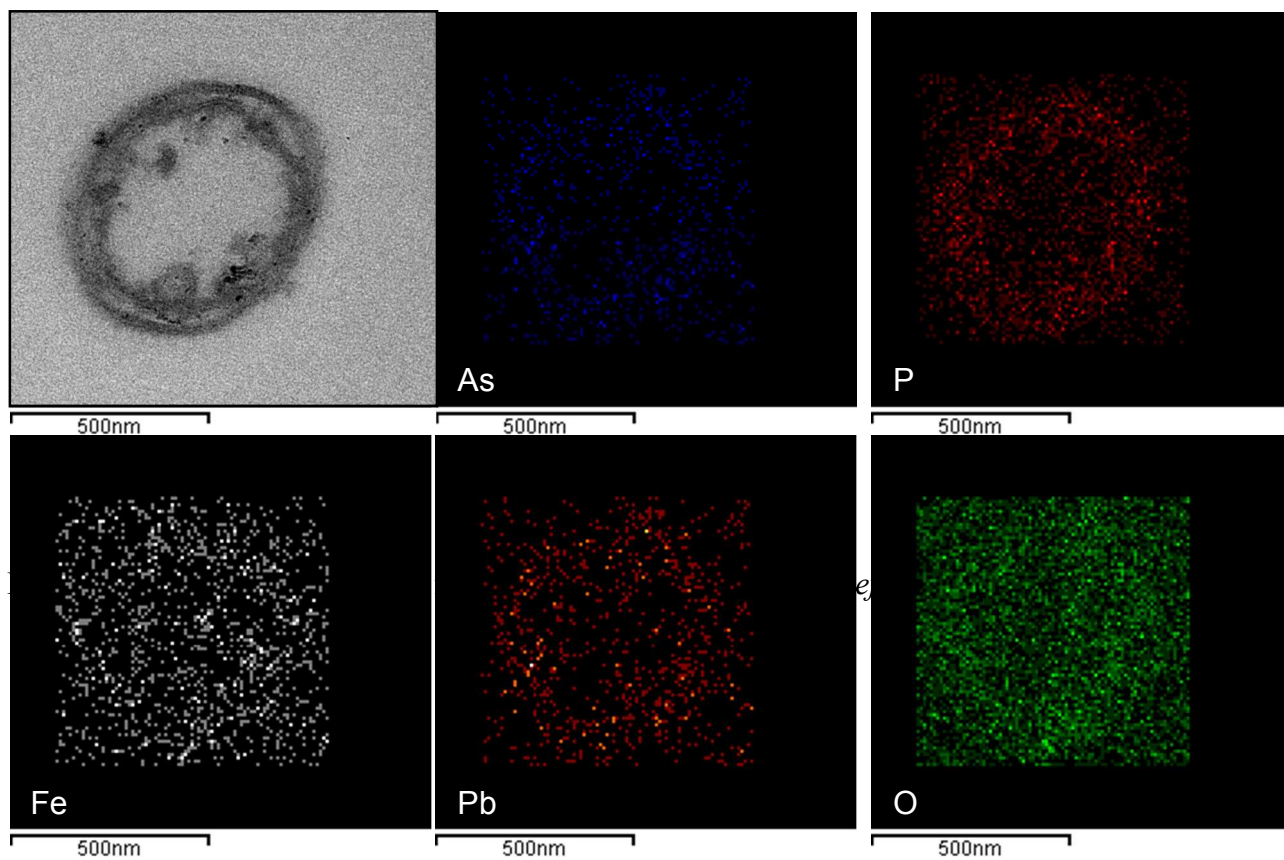


Figure S9. TEM-EDS elemental maps of a cross sectioned *S. putrefaciens* cell at 336 hours.

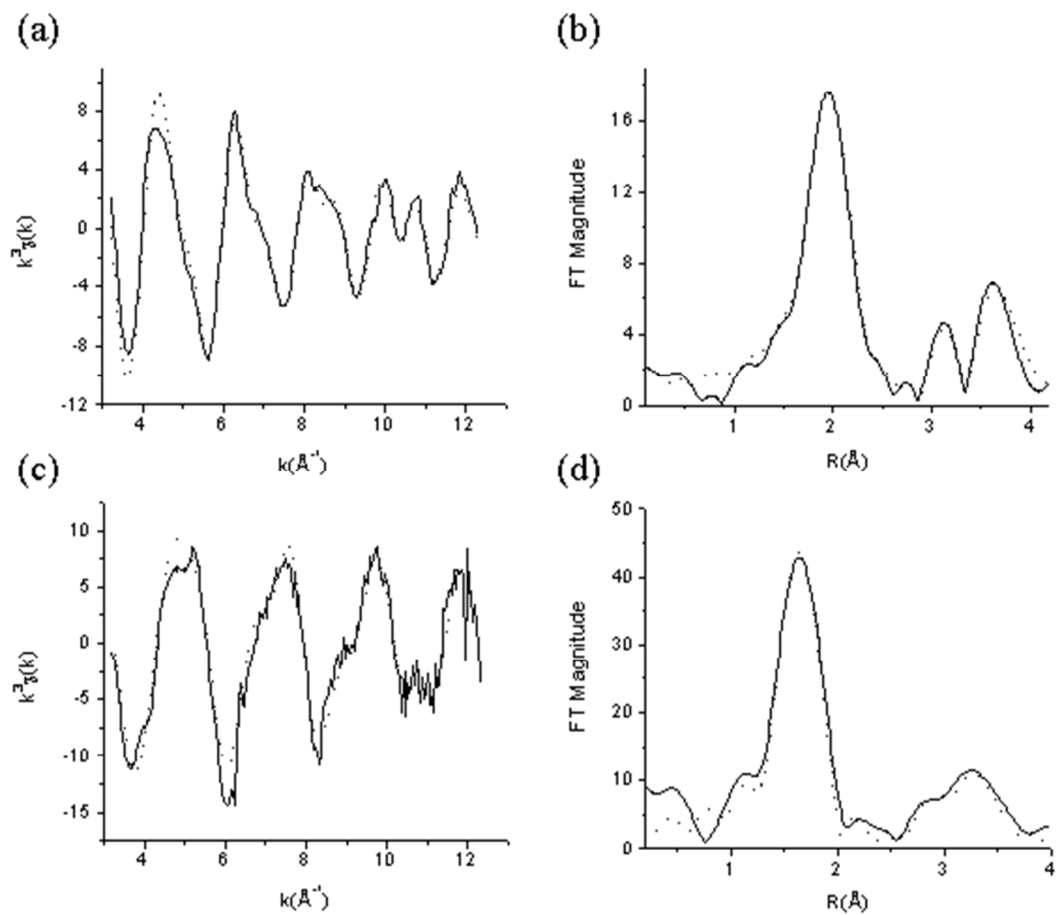


Figure S10. (a) Fitted Fe K-edge EXAFS and (b) associated FT. In (c) and (d) are shown the fitted As K-edge EXAFS and FT of the unreacted Pb-As jarosite.

S1 References:

1. Binsted, N.; Gurman, S.; Campbell, J.; Stephenson, P., SERC Daresbury Laboratory Program EXCURVE. *Warrington, UK* **1991**.
2. Sherman, D. M.; Randall, S. R., Surface complexation of arsenic (V) to iron (III)(hydr) oxides: structural mechanism from ab initio molecular geometries and EXAFS spectroscopy. *Geochim. Cosmochim. Acta* **2003**, *67*, (22), 4223-4230.
3. Rehr, J.; Albers, R., Scattering-matrix formulation of curved-wave multiple-scattering theory: Application to x-ray-absorption fine structure. *Physical Review B* **1990**, *41*, (12), 8139.
4. Rehr, J.; Albers, R.; Zabinsky, S., High-order multiple-scattering calculations of x-ray-absorption fine structure. *Physical Review Letters* **1992**, *69*, (23), 3397.
5. Fendorf, S.; Eick, M. J.; Grossl, P.; Sparks, D. L., Arsenate and chromate retention mechanisms on goethite. 1. Surface structure. *Environ. Sci. Technol.* **1997**, *31*, (2), 315-320.
6. Koningsberger, D.; Mojet, B.; Van Dorssen, G.; Ramaker, D., XAFS spectroscopy; fundamental principles and data analysis. *Topics in catalysis* **2000**, *10*, (3), 143-155.
7. Menchetti, S.; Sabelli, C., Crystal chemistry of the alunite series: crystal structure refinement of alunite and synthetic jarosite. *Neues Jahrbuch Mineralogie Monatshefte, H* **1976**, *9*, 406-417.
8. Savage, K. S.; Bird, D. K.; O'Day, P. A., Arsenic speciation in synthetic jarosite. *Chem. Geol.* **2005**, *215*, (1), 473-498.
9. Robie, R. A.; Hemingway, B. S., Thermodynamic properties of minerals and related substances at 298.15 K and 1 bar (10^5) pascals pressure and higher temperature. *U.S. Geological Survey* **1995**, *Bulletin 2131*.
10. Shock, E. L.; Helgeson, H. C., Calculation of the thermodynamic and transport properties of aqueous species at high pressures and temperatures: Correlation algorithms for ionic species and equation of state predictions to 5 kb and 1000 °C. *Geochim. Cosmochim. Acta* **1988**, *52*, (8), 2009-2036.
11. Stumm, W.; Morgan, J. J., *Aquatic Chemistry: Chemical Equilibria*. John Wiley and Sons, Inc.: New York, 1996.
12. Wagman, D. D. *The NBS tables of chemical thermodynamic properties. Selected values for inorganic and C1 and C2 organic substances in SI units*; DTIC Document: 1982.
13. Amend, J. P.; Shock, E. L., Energetics of overall metabolic reactions of thermophilic and hyperthermophilic Archaea and Bacteria. *Fems Microbiol. Rev.* **2001**, *25*, (2), 175-243.
14. Nordstrom, D.; Archer, D., Arsenic thermodynamic data and environmental geochemistry. *Arsenic in ground water* **2003**, 1-25.

